2D-Rectangular *c2mm* mesoporous silica nanoparticles with tunable elliptical channels and lattice dimensions†‡

Chia-Min Yang,*[a] Ching-Yi Lin,[a] Yasuhiro Sakamoto,[b] Wei-Chia Huang[a] and Li-Ling Chang[a]

Received (in Cambridge, UK) 30th July 2008, Accepted 23rd September 2008
First published as an Advance Article on the web 9th October 2008
DOI: 10.1039/b812967c

Mesoporous silica nanoparticles with a two-dimensional center-rectangular (plane group *c2mm*) lattice and coiled elliptical channels have been synthesized; the new synthetic route also allows simple control over the lattice dimensions and the elliptical shape of the channels.

Most surfactant-templated mesoporous materials[1,2] display pore topologies closely related to those for the liquid-crystal-like phases typical of surfactant–water systems.[1–5] Among them, the materials (for example, SBA-8)[6] with a two-dimensional (2D) centered-rectangular (plane group *c2mm*) lattice, correlated to the ribbon-intermediate phases, may be regarded as deformed structures of the hexagonal mesophase in which the cylindrical micelles are flattened.[7–9] The elliptical channels resulting from the structural deformation are of special interest because of the additional anisotropy of the channels, but it remains a challenge to discover new synthetic strategies to control and extend the degree of the structural deformation. Here we report the synthesis of *c2mm* mesoporous silica nanoparticles with tunable lattice dimensions and tunable elliptical channel section. In addition, the elliptical channels are coiled, forming helical secondary mesostructure. The synthesis is envisioned to bring unprecedented opportunities to explore curvature-dependent chemistry of inclusion and surface functionalization[10–12] in the anisotropic channel space.

The synthesis was performed in a dilute solution of cetyltrimethylammonium bromide (CTAB) and tetraethylene glycol dodecyl ether ($C_{12}EO_4$) using tetraethoxysilane (TEOS) as a silica source and sodium hydroxide (NaOH) as a base catalyst. The molar composition of the synthesis mixture was $8 : f_n : (1 - f_n) : 2.56 : 9840$ TEOS : $C_{12}EO_4$: CTAB : NaOH : H_2O, where f_n is the molar fraction of $C_{12}EO_4$ in the surfactant mixture. Fig. 1 shows the X-ray diffraction (XRD) patterns of the mesophases synthesized with varied f_n. In the absence of $C_{12}EO_4$, the material was essentially hexagonal MCM-41.[1,2] As indexed with a rectangular lattice (*cf.* Fig. 1), the ratio of the unit cell parameters a and b is $\sqrt{3} \sim 1.73$. The hexagonal structure remained when a small amount of $C_{12}EO_4$ ($f_n < 0.15$) was applied, but the corresponding reflections shifted toward a lower angle and became slightly broader. As f_n increased from 0.15 to 0.35, however, the peak originally attributed to the 10 reflection of the *p6mm* structure evolved and split into two, accompanied by the shifts of other high-order reflections. These XRD patterns could be perfectly indexed assuming a *c2mm* symmetry. For $f_n = 0.15$, the first peak was asymmetric and could be deconvoluted and indexed as the 20 and 11 reflections of a *c2mm* structure. With increasing f_n from 0.15 to 0.35, the parameter b became slightly smaller while the parameter a increased from 8.7 nm to 11.2 nm, resulting in an increase of the a/b ratio from 1.85 to 2.73. Adding more $C_{12}EO_4$ resulted in materials with lamellar or disordered structure, as evidenced by the XRD pattern of the material synthesized with $f_n = 0.40$. The results clearly show that the hexagonal structure is transformed to *c2mm* mesophases which can be modulated by simply adjusting the molar fraction of $C_{12}EO_4$.

The *c2mm* materials, designated as MMT-1, and other surfactant–silica mesophases were calcined to remove

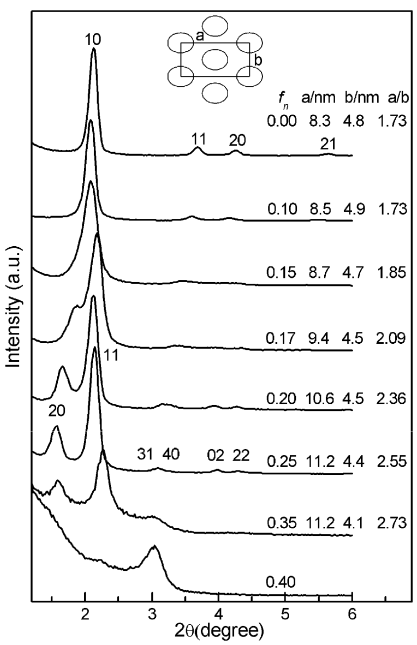

Fig. 1 XRD patterns of the surfactant–silica mesophases synthesized with different surfactant ratios.

[a] *Department of Chemistry, National Tsing Hua University, Hsinchu 30013, Taiwan. E-mail: cmyang@mx.nthu.edu.tw; Fax: +886 3 5165521; Tel: +886 3 5731282*
[b] *Structural Chemistry, Arrhenius Laboratory, Stockholm University, S-10691 Stockholm, Sweden*

† This paper is dedicated to Professor Kuei-Jung Chao on the occasion of her retirement.

‡ Electronic supplementary information (ESI) available: Experimental details, structural properties derived from N_2 physisorption data, XRD pattern, SEM image and time-resolved SAXS patterns and data. See DOI: 10.1039/b812967c

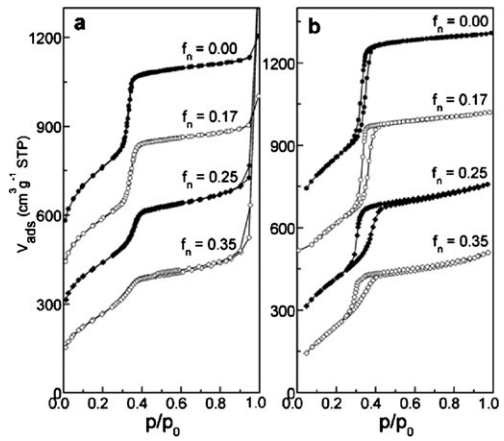

Fig. 2 Nitrogen (a) and argon (b) physisorption isotherms at 77 K for the mesoporous silica materials synthesized with varied f_n.

surfactants, during which the MMT-1 materials experienced larger contractions along the *a* direction and thus have slightly smaller *a*/*b* ratios than the as-synthesized materials (ESI‡). The MMT-1 materials are expected to possess channels with a different elliptical section which may reflect the shape of the hysteresis loop in gas physisorption isotherms.[13] Fig. 2a shows nitrogen physisorption isotherms of mesoporous materials synthesized with f_n = 0 (MCM-41), 0.17, 0.25 and 0.35, and the derived structural properties are listed in ESI‡. All the isotherms are type IV curves showing steps over the relative pressure range of 0.25–0.4, and the step becomes smaller and wider with increasing f_n from 0 to 0.35. The isotherms do not exhibit any hysteresis loops, as expected for mesochannels with diameters <4 nm (at 77 K the pore fluid is above the so-called hysteresis critical temperature).[13] On the other hand, argon physisorption at 77 K makes it possible to choose a thermodynamic range for the confined fluid where hysteresis can occur and may in turn make it possible to obtain information about the pore shape. Indeed, MCM-41 exhibits a narrow H1-type hysteresis loop associated with the capillary condensation in uniform cylindrical mesopores (Fig. 2b).[14] Interestingly, the loop becomes wider for the sample with f_n = 0.17, and it is transformed into H2-type loops for those with f_n = 0.25 and 0.35. The H2-type loops may support the assumption of an elliptical pore shape in the MMT-1 with large deformation because a delay in the evaporation of the condensed liquid could happen in the channel-type mesopores that exhibit constrictions in pore diameter along the pore axis.[13]

The *c2mm* MMT-1 synthesized with f_n = 0.25 was further characterized. A scanning electron microscopy image shows that the sample consists of uniform particles with diameters of 150–200 nm (ESI‡). High-resolution transmission electron microscopy (HRTEM) reveals fascinating structural features of this material. The elliptical shape of the channels arranged in a *c2mm* symmetry can be clearly observed (Fig. 3a), and the major and minor axes of the pore section are estimated to be 4.0 nm and 2.8 nm, respectively. Moreover, the elliptical channels are wound around a center axis parallel to the minor axis of the elliptical pore section (indicated by the arrows in Fig. 3a), and center singularity can be observed in the image viewed along the axis (Fig. 3b). The arrangement of the

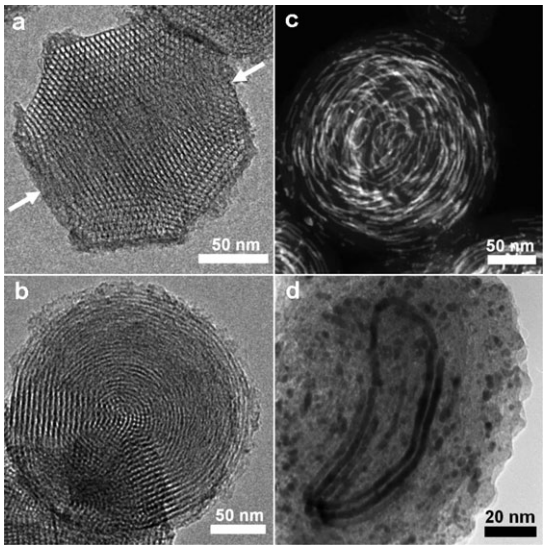

Fig. 3 (a) and (b) HRTEM images of the MMT-1 materials synthesized with f_n = 0.25. (c) DF-STEM of the Pt-infiltrated MMT-1. (d) TEM images of the Pt-infiltrated MMT-1 showing a helical Pt nanowire.

elliptical channels was further confirmed by dark-field scanning transmission electron microscopy (DF-STEM) images of the platinum-infiltrated MMT-1 material (Fig. 3c). The elliptical channels could be either closed-off rings or helices; the latter seems to be the case suggested by the TEM image of a helical Pt nanowire in MMT-1 (Fig. 3d). The observed helical pitch is very low, probably just one or a few lattice constants, and it could also explain why the rectangular channel arrangement is visible on both edges of the nanoparticles.

The formation of the MMT-1 synthesized with f_n = 0.25 was also studied by time-resolved small-angle X-ray scattering (SAXS).[15] A mesostructured phase was formed at about 19 min after adding TEOS, suggested by the appearance of a Bragg reflection (q = 0.134 Å^{-1}) corresponding to a d-spacing of 4.7 nm (Fig. 4). The same induction time was observed for

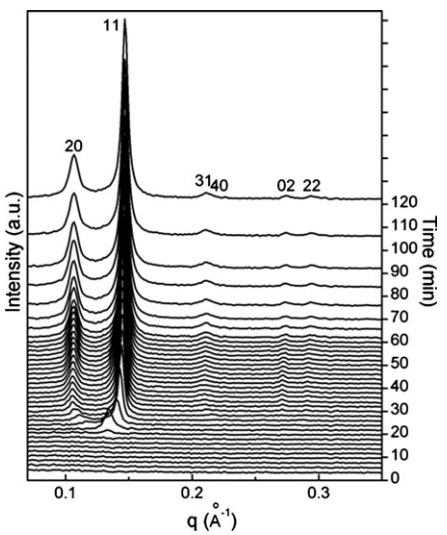

Fig. 4 Time-resolved SAXS patterns of the MMT-1 material synthesized with f_n = 0.25.

MCM-41 (ESI‡). For MMT-1, however, the reflection evolved and split immediately after its appearance, and the two reflections continued to sharpen, increase in intensity and move away from each other. Additional high-ordered reflections appeared at a reaction time of 30 min and remained in position after that. The patterns could be indexed assuming a 2D-rectangular lattice. The fact that the a/b ratio increased from 1.73 to 2.57 within $\sim$10 min (ESI‡) clearly shows a rather rapid structural deformation within that period.

The observed structural deformation should be associated with the strong cooperative interactions between the anionic silicate species and the cationic surfactant at the synthesis pH ($\sim$pH 10.5).[16,17] On the other hand, the nonionic $C_{12}EO_4$ molecules were also incorporated in the as-synthesized mesophases. The molar ratios of the two surfactants in the as-synthesized mesophases were almost identical to the corresponding values in the synthesis solutions for f_n = 0.15–0.30, suggested by the relative amounts of the nitrogen (from CTAB) and the oxygen (from $C_{12}EO_4$) in the surfactant mixture extracted from them by the elemental analysis. The presence of $C_{12}EO_4$ may reduce the curvature of the micelles,[3,4] and it has been applied to synthesize MCM-48 mesophase from concentrated surfactant mixtures.[18] For MMT-1 synthesized in dilute surfactant solutions, we speculate that the condensation of the silicate species adsorbed preferentially onto the cetyltrimethylammonium (CTA) cations might induce a segregation of the two surfactants (*cf*. Scheme 1), similar to that observed in a ribbon-like liquid crystal formed by mixed amphiphiles with polar heads of differing nature.[19] The segregated $C_{12}EO_4$ might form the flattened parts of the deformed rod-like micelles in the surfactant–silica mesophase with more silicate species around the highly curved parts of the elliptical micellar rods where CTA are concentrated. The micellar rods elongate and may start to coil into a helical mesostructure to reduce the surface energy. In principle, the rods could coil around the axis either parallel or perpendicular to the minor axis of the ellipse. The former case was observed exclusively in the MMT-1 materials, and it might be associated with further condensation of the silica species at the highly curved positions of the elliptical micellar rods.

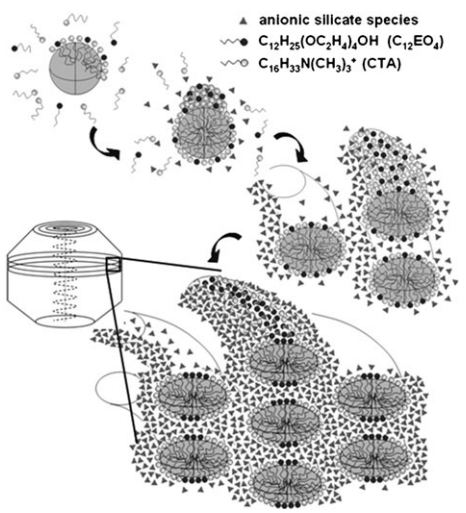

Scheme 1 A proposed formation mechanism of the *c2mm* MMT-1 materials.

The kinetically driven structural deformation observed in the synthesis of MMT-1 materials is completely different from that induced by anisotropic contraction in mesostructured films.[20,21] On the other hand, SBA-8 and the so-called M_α mesophase also possess *c2mm* structure.[6] The structure of SBA-8 deforms along a different direction and the a/b ratio of SBA-8 is smaller than $\sqrt{3}$. However, their degrees of structural deformation are small and could not be modulated as in the case of MMT-1 materials.

The authors thank U. S. Jeng, Y. H. Lai, H. S. Sheu and W. T. Chuang (NSRRC) for their help with SAXS measurements, M. Thommes and B. Zibrowius for beneficial discussions, and the National Science Council of the Republic of China for financial support under the contract no. NSC95-2113-M-007-032-MY. YS thanks the Swedish Research Council (VR) for financial support.

Notes and references

1 C. T. Kresge, M. E. Leonowicz, W. J. Roth, J. C. Vartuli and J. S. Beck, *Nature*, 1992, **359**, 710.
2 J. S. Beck, J. C. Vartuli, W. J. Roth, M. E. Leonowicz, C. T. Kresge, K. D. Schmitt, C. T.-W. Chu, D. H. Olson, E. W. Sheppard, S. B. McCullen, J. B. Higgins and J. L. Schlenker, *J. Am. Chem. Soc.*, 1992, **114**, 10834.
3 Q. Huo, D. Margolese, U. Ciesla, P. Feng, T. E. Gier, P. Sieger, R. Leon, P. Petroff, F. Schüth and G. D. Stucky, *Nature*, 1994, **368**, 317.
4 A. Firouzi, D. Kumar, L. M. Bull, T. Bessier, P. Sieger, Q. Huo, S. A. Walker, J. A. Zasadzinski, C. Glinka, J. Nicol, D. Margolese, G. D. Stucky and B. F. Chmelka, *Science*, 1995, **267**, 1138.
5 S. Che, A. E. Garcia-Bennett, T. Yokoi, K. Sakamoto, H. Kunieda, O. Terasaki and T. Tatsumi, *Nat. Mater.*, 2003, **2**, 801.
6 D. Zhao, Q. Huo, J. Feng, J. Kim, Y. Han and G. D. Stucky, *Chem. Mater.*, 1999, **11**, 2668.
7 F. Husson, H. Mustacchi and V. Luzzati, *Acta Crystallogr.*, 1960, **13**, 668.
8 H. Hagslätt, O. Söderman and B. Jönsson, *Liq. Cryst.*, 1992, **12**, 667.
9 S. Gustafsson, P. Q. Quist and B. Halle, *Liq. Cryst.*, 1995, **18**, 545.
10 M. K. Kidder, P. F. Britt, Z. Zhang, S. Dai, E. W. Hagaman, A. L. Chaffee and A. C. Buchanan III, *J. Am. Chem. Soc.*, 2005, **127**, 6353.
11 Y. Yang, G. Du, S. Lim and G. L. Haller, *J. Catal.*, 2005, **234**, 318.
12 O. Petrov and I. Furó, *Phys. Rev. E: Stat. Phys., Plasmas, Fluids, Relat. Interdiscip. Top.*, 2006, **73**, 011608.
13 S. Lowell, J. E. Shields, M. A. Thomas and M. Thommes, *Characterization of Porous Solids and Powders: Surface area, Pore size and Density*, Kluwer Academic Publishers, Dordrecht, 2004.
14 P. J. Branton, P. G. Hall, K. S. W. Sing, H. Reichert, F. Schüth and K. K. Unger, *J. Chem. Soc., Faraday Trans.*, 1994, **90**, 2965.
15 Y. C. Hsu, Y. T. Hsu, H. Y. Hsu and C. M. Yang, *Chem. Mater.*, 2007, **19**, 1120.
16 C. J. Brinker and G. W. Scherer, *Sol-Gel Science*, Academic Press, San Diego, 1990.
17 J. N. Israelachvili, *Intermolecular & Surface Forces*, Academic Press, London, 1991.
18 R. Ryoo, S. H. Joo and J. M. Kim, *J. Phys. Chem. B*, 1999, **103**, 7435.
19 S. Alpérine, Y. Hendrikx and J. Charvolin, *J. Phys. Lett.*, 1985, **46**, 27.
20 D. A. Doshi, N. K. Huesing, M. Lu, H. Fan, Y. Lu, K. Simmons-Potter, B. G. Potter, Jr, A. J. Hurd and C. J. Brinker, *Science*, 2000, **290**, 107.
21 M. Klotz, P.-A. Albouy, A. Ayral, C. Ménager, D. Grosso, A. Van der Lee, V. Cabuil, F. Babonneau and C. Guizard, *Chem. Mater.*, 2000, **12**, 1721.